USING AN EMISSIVE PROBE TO MEASURE TIME-AVERAGED PLASMA POTENTIAL IN A HALL THRUSTER DISCHARGE

A. Pétin[1]*, J. Vaudolon[1], S. Mazouffre[1], P. Kudrna[2], M. Tichý[2],

[1] ICARE, CNRS, 1C Avenue de la Recherche Scientifique, 45071 Orléans, France
[2] Charles University, Faculty of Mathematics and Physics, Prague, Czech Republic
*aude.petin@cnrs-orleans.fr

ABSTRACT

An emissive probe is a easily-built, smart and efficient diagnostics for measuring both the plasma and the floating potential. For maxwellian electrons, an estimation of the electron temperature can be deduced from the previous quantities. Measurements are performed in the plume of a Hall thruster in order to define the limit of this diagnostics and to optimize it. Finally a comparison with LIF measurements is performed.

1. INTRODUCTION

An electron emitting probe is a complementary idea to the electron collecting probe; both of them have been proposed by Langmuir in 1923 [1]. Compared with the collective Langmuir probe, the main advantage of the emissive probe is that no sweep of the probe voltage is required. Then, an emissive probe provides direct spatially or time-resolved measurements of the plasma and the floating potentials [2].
Measurements have been performed in the plume of a Hall thruster (HT). A HT is an advanced electrical propulsion device mainly used on geosynchronous satellites for orbit corrections and station keeping. In a HT, a low pressure ExB discharge is generated. Since only electrons are sensitive to the magnetic field (B), a charge separation appears and increases the electric field (E) which is at the origin of the ion acceleration and then at the origin of the thrust.
Such a plasma hardly sputters any in-situ diagnostics and decreases dramatically its lifetime. Direct measurements with an emissive probe have been performed thanks to a compact, fast movable piezo-electrical stage [3]. The disturbance of the plasma due to the probe is studied in order to optimize the trajectory of the probe in the discharge. The profile of the plasma potential is compared to the plasma potential deduced from LIF measurements.

2. EXPERIMENTAL SETUP

2.1 The emissive probe

An emissive probe consists in a low work-function material, immersed in the plasma, heated until it reaches its electrons emission point. In a previous paper, Sheehan and Hershkowitz exhaustively described the various manners for obtaining the plasma potential and presented several ideas for the probe design and the heating methods, see [4]. In this paper, we focus on the single method available to get a direct measurement of the plasma potential, i.e the method of the floating point [5] [6]. This method is based on the well-known expression of the plasma potential to which a term of emitting electron current I_{ee} is added. Assuming maxwellian electrons and cold ions, this expression becomes:

$$V_p = V_{fl} - T_e \ln\left(\frac{I_{s,e}}{I_{s,i} + I_{ee}}\right) \qquad (1)$$

where $I_{s,e}$ and $I_{s,i}$ are the electron and ion saturation currents and T_e is the electron temperature (eV). The increase of the electron emission leads to the suppression of the last term when I_{ee}=$I_{s,e} >> I_{s,i}$. Then the floating potential approaches the plasma potential and ideally reaches it. Figure 1 shows the floating potential of the probe as a function of the heating current. The ideal plateau at large current is replaced by a slow increase of the probe potential. The change of slope gives the heating current (about 4.5 A) associated with the plasma potential. However, emitted electrons are colder than plasma electrons, which induce a space charge effect around the probe. The plasma potential "seen" by the

probe becomes lower than the true plasma potential, inducing its underestimation. An other cause of underestimation has been argued by Kempf and Sellen : below plasma densities of $10^5 cm^{-3}$ the electron saturation current is small enough to make space charge effect significant. In the case of dense plasma (above $10^{12} cm^{-3}$), melting of the filament appears to be an other problem. However, in this range of densities ($10^5 cm^{-3}$ - $10^{12} cm^{-3}$), the emissive probe seems to be a pertinent and easy-usable diagnostics. Several uncertainties are associated to this diagnostics. The most important seems to be the fact that an emissive probe in the limit of large emission will float 1.5 T_e below the plasma potential.

The emitting part of the probe consists in a 6 mm length and 0.15 mm in diameter loop of thoriated tungsten wire mechanically connected to two different copper wires. The coper wires are slipped in an alumina double-drilled tube of 10 cm in length and 3 mm in diameter. Each copper wire is connected to a pole of a power supply in order to get a heating circuit. Finally, the plasma potential is measured at the middle point of a voltage divider bridge which makes the circuit symmetrical.

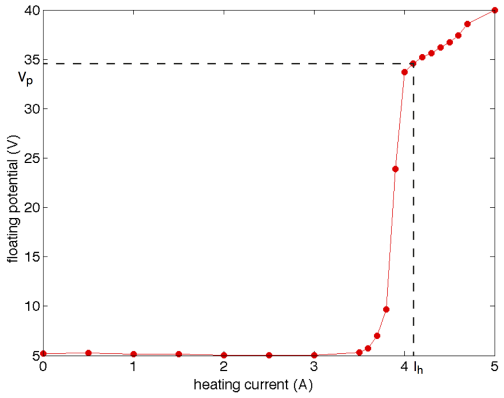

Fig. 1: Heating characteristic of an emissive probe : floating probe potential as a function of heating current. The curve was obtained in the 200W-class Hall thruster, on the channel axis, at 6 mm from the thruster exit plan.

2.2 Hall thruster and test bench

Experiments discussed in this paper have been performed in the plume of a 200 W-class Hall thruster. This thruster delivers a 10 mN thrust when operating a 250V and 1.0 mg/s Xenon mass flow rate, see [7]. A heated hollow cathode with LaB_6 element is used as a source of electrons with a Xenon mass flow rate of 0.2 mg/s. The test bench consists of a cylindrical stainless-steel vacuum chamber of dimensions 1.8 m in length and 0.8 m in diameter. It is equipped with a three-stage pumping system composed of a dry pump (400m^3/h), a 200 l/s turbomolecular pump and a cryogenic pump whose surface temperature reaches about 35K. The typical chamber pressure during experiments is about 10^{-5} mbar-N_2.

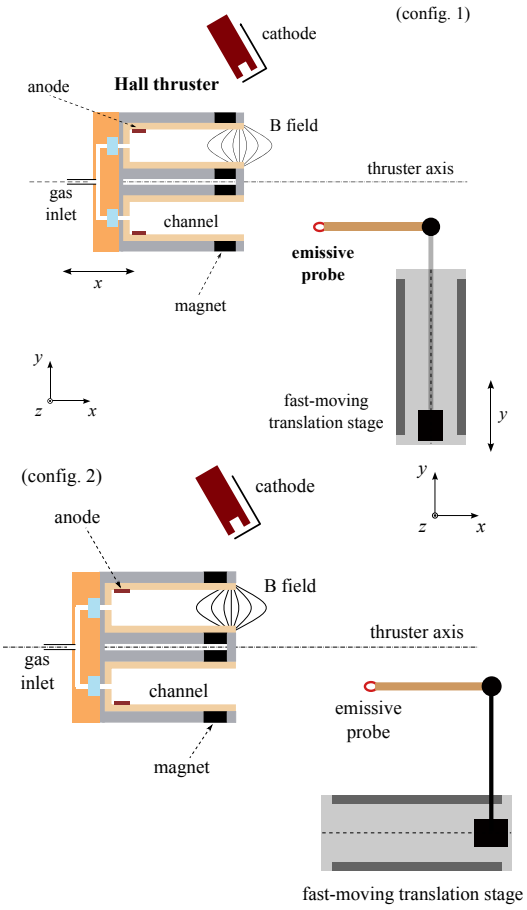

Fig. 2: Picture of the two configurations of the probe shifting.

The high particles flux in the near-field plasma strongly decreases the lifetime of the probe. Then, measurements were performed thanks to a fast-moving stage, see [3]. This stage is the PILine® Linear Motor Stage M664K018. This linear drive reaches a maximum velocity of 350 mm/s and maximum acceleration and deceleration of 2000 mm/s^2. Its dimensions are 140 × 63 × 14 mm. The linear stage has a travel range of 90 mm (45 mm on both side). Furthermore, it is vacuum compatible down to 10^{-6} mbar.

In addition to the piezo stage, the thruster is set up on two movable stages allowing two degree of freedom x and y, see Fig. 2. Finally, the piezo stage is mounted on a manual stage in z direction.

3. TIME-AVERAGED MEASUREMENTS

3.1 Disturbances induced by the probe

The 200W-class thruster is a small dimension thruster. The emissive probe dimensions (3 mm in diameter and 10 cm in length) cannot be neglected compared to thruster sizes. As long as the emissive probe is used far from the exit plan, disturbances are negligible; they become significant when approaching the thruster [8]. These disturbances appear to be due to (1) the sputtering of the alumina tube and the probe support (aluminum rod), (2) the heating of the probe (electron emission) and (3) the secondary electron emission from the alumina tube. In all cases, these disturbances correspond to an increase of the discharge current (I_d) and a decrease of the cathode potential to ground (V_{crp}). Disturbances associated to both travel directions of the probe have been observed. In the first case, the piezo stage is used to move the probe in y direction and the thruster stage permits an increment in the x direction, see Fig. 2, config. 1. In the second case, the piezo stage is used to move the probe in x direction since the thruster stage sets the y position, see config. 2. For each case, the probe axis is parallel to the thruster axis in order to limit the sputtering of the alumina tube. The main advantage of the config. 2 is to allow the determination of the plasma potential inside the thruster channel. During its shifting, the probe movement gets a phase of acceleration, of constant velocity (350 mm/s) and of deceleration whereas the oscilloscope recording is regular in time. Then, oscilloscope sampling is not spacially regular. In order to correlate oscilloscope data to the probe travel, a trigger was sent by the piezo controller as soon as the probe have moved over 0.5 mm. Figure 3 on top and bottom show respectively the discharge current as a function of the probe position in the case of the first and second experiment. In the top figure, the abscissa gives the y position normalized by the medium radius of the channel thruster : y=0 correspond to the thruster axis and y=1 and y=-1 to the channel center. In the second figure, x=0 corresponds to the position of the exit plane. Data in Fig. 3 has been recorded with a sampling of 100000 (top panel) and 45405 (bottom panel) respectively for a probe travel 90 mm. Data processing consist in a smoothing over 250 (respectively 500) points. Experiments have been performed for a discharge voltage of 200 V and an Xenon anode mass flux of 1mg/s.

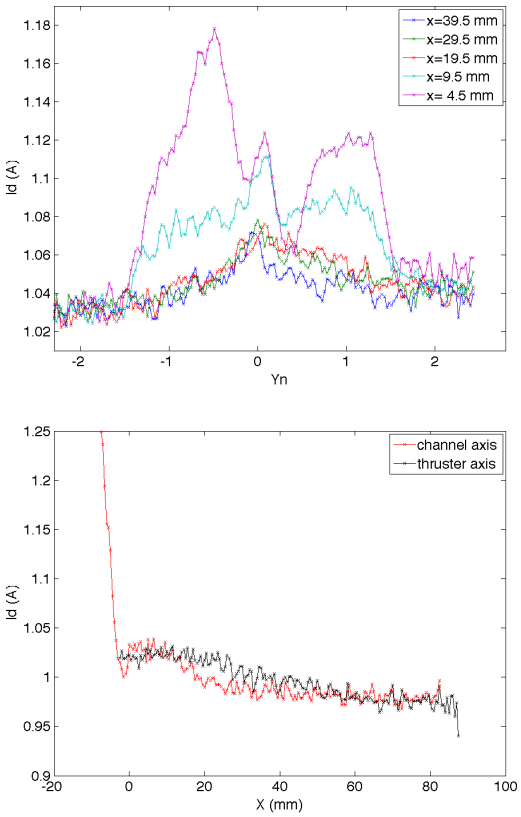

Fig. 3: On top: Discharge current as a function of y direction normalized to the channel medium radius (config. 1). Several x positions are shown. On bottom: Discharge current as a function of the probe position x. x=0 corresponds to the thruster exit plan (config. 2). Two y positions are presented : the thruster axis and the channel axis.

Increase of I_d is well observed. On the channel axis it appears that moving the probe along the y direction induces large disturbances in the very close proximity of the thruster: at 4.5 mm, I_d increases of 8 % of disturbance for config. 1 against 5 % for config. 2. However, after 1 cm far from the thruster and considering an error bar of about 1-2% which is the amplitude of the discharge current oscillation (depending of the distance), the disturbances can be considered similar. On the thruster axis, disturbances are fairly equivalent close to the thruster since moving farther, the config. 1 appears the worst case. : at 39.5 mm, 4% of increase for the config. 1 against 0.4 % for the config. 2. Figure 3 shows that maximal disturbances do not appear on the channel or thruster axis, like expected. A maximum of 14.4 % is reached at y=-0.49, i.e. 9 mm from the channel axis. This break of symmetry certainly originates from the sputtering of not only the emissive probe but of all the set up, including the metallic rod. Then the maximum is not obtained in the case of the probe onto the channel axis but in the case where the plasma "sees" the

largest part of the set up. Finally, the disturbance induce by the probe inside the channel (config. 2) is about 27.4 % at the probe stop for x=-7.5 mm. That is the worst case since the probe just stops. For x=-4 mm, disturbance is only about 7 % !

Another experiment (config. 1) showed that the probe heating induces an increase of I_d on the channel axis, when the probe is close to the thruster ($\approx$ 3% at x=4 mm) and on the thruster axis, on a longer distance (5% on the thruster axis at x=20 mm).

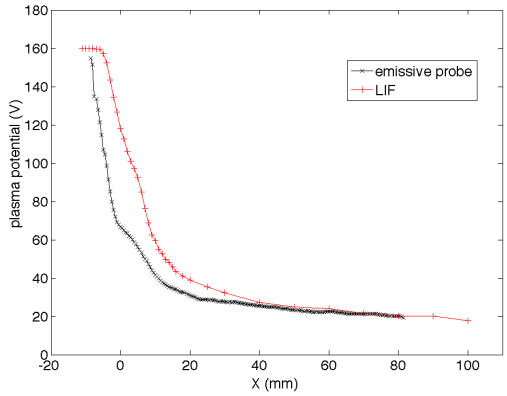

Fig. 4: Profile of the plasma potential along channel axis obtained with an emissive probe and by LIF. The thruster power was about 200W, anode mass flow rate 1mg/s, the potential of the cathode to ground about -20V, the maximum of the magnetic field 250G, the gas was Xenon

3.2 Comparison with other diagnostics

In the far-field of this thruster, measurements of the plasma potential with an emissive probe have been already compared to Langmuir probe [9]. Near and inside the thruster, measurements have been performed under identical operating conditions with an emissive probe and by LIF in order to compare them. Contrary to emissive probes, LIF does not provide a direct measurement of the plasma potential, but a measurement of the acceleration potential experienced by the ions. This potential can be an approximation of the plasma potential with a maximal error bar of 1V when the electric field becomes weak. The error bar in the acceleration area (i.e. from -5 mm inside the channel to 10 cm outside) is 0.5V. A description of the LIF technique and set up is given in [10]. Plasma potential on the channel axis is presented in Fig. 4 for the two diagnostics as a function of the distance from the thruster. LIF plot is voltage shifted in order to obtain the same potential as emissive probe's for the farther record data from the thruster (x= 80 mm). Similar behavior of the plasma potential is found, particularly the local little increase at about x=6 mm. However, from x=30 mm a gap appears between the two diagnostics and the potential from LIF become higher than the potential from emissive probe. The largest gap corresponds to a underestimation of the LIF potential by the emissive probe of about 55%, at x=-1mm inside the channel. Furthermore, since the LIF's potential stabilizes at 160V, that is not the case of the emissive probe's potential in the spatial range of record. The underestimation of the plasma potential by the emissive probe originates from both the high electron temperature in the thruster acceleration area and perhaps from the plasma disturbance due to the probe.

4. Conclusion

The emissive probe diagnostics is used in a 200W-class Hall thruster. Disturbance due to the probe are studied . A fast movable piezo stage is used in order to decrease them and increase the lifetime of the probe. Plasma potential determined by the emissive probe is compared with LIF measurements.

REFERENCES

[1] I. Langmuir, *J. Franklin Inst.*, 196, 751-62

[2] S. Mazouffre et al., IEEE Trans. Plasma Sci., in press, 2014

[3] K. Dannenmayer and S. Mazouffre, Rev. Sci. Instrum., **83**,123503, 2012

[4] J. P. Sheehan and N. Hershkowitz, Plasma Sources Sci. Technol., **20**, 1-2, 2011

[5] R. F. Kempf and J. M. Sellen, Rev. Sci. Instrum., **37**, 455, 1966

[6] M. A. Makowski and G. A. Emmert, Rev. Sci. Instrum., **54**, 830, 1983

[7] S. Mazouffre et al., J. Phys. D: Appl. Physics , **45**, 185203, 2012

[8] D. Staack et al., AIAA proceedings, 4109, 2002

[9] K. Dannenmayer et al., Plasma Sources Sci. Technol., **20**, 055020, 2012

[10] S. Mazouffre, Plasma sources Sci. Technol., **22**, 013001, 2013